Harnessing RNAi-based nanomedicines for therapeutic gene silencing in B-cell malignancies

Shiri Weinstein[a,b,c,1], Itai A. Toker[a,b,c,1], Rafi Emmanuel[a,b,c], Srinivas Ramishetti[a,b,c], Inbal Hazan-Halevy[a,b,c], Daniel Rosenblum[a,b,c], Meir Goldsmith[a,b,c], Avigdor Abraham[d], Ohad Benjamini[d], Osnat Bairey[e], Pia Raanani[e], Arnon Nagler[d], Judy Lieberman[f,g], and Dan Peer[a,b,c,2]

[a]Laboratory of NanoMedicine, Department of Cell Research and Immunology, George S. Wise Faculty of Life Sciences, Tel Aviv University, Tel Aviv 6997801, Israel; [b]Department of Materials Science and Engineering, the Iby and Aladar Fleischman Faculty of Engineering, Tel Aviv University, Tel Aviv 6997801, Israel; [c]Center for Nanoscience and Nanotechnology, Tel Aviv University, Tel Aviv 6997801, Israel; [d]Division of Hematology and Oncology, Sheba Medical Center, Tel Hashomer 5262100, Israel; [e]Institute of Hematology, Rabin Medical Center, Petah Tikva 4941492, Israel; [f]Program in Cellular and Molecular Medicine, Boston Children's Hospital, Harvard Medical School, Boston, MA 02115; and [g]Department of Pediatrics, Harvard Medical School, Boston, MA 02115

Edited by Mark E. Davis, California Institute of Technology, Pasadena, CA, and approved December 4, 2015 (received for review September 28, 2015)

Despite progress in systemic small interfering RNA (siRNA) delivery to the liver and to solid tumors, systemic siRNA delivery to leukocytes remains challenging. The ability to silence gene expression in leukocytes has great potential for identifying drug targets and for RNAi-based therapy for leukocyte diseases. However, both normal and malignant leukocytes are among the most difficult targets for siRNA delivery as they are resistant to conventional transfection reagents and are dispersed in the body. We used mantle cell lymphoma (MCL) as a prototypic blood cancer for validating a novel siRNA delivery strategy. MCL is an aggressive B-cell lymphoma that overexpresses cyclin D1 with relatively poor prognosis. Down-regulation of cyclin D1 using RNA interference (RNAi) is a potential therapeutic approach to this malignancy. Here, we designed lipid-based nanoparticles (LNPs) coated with anti-CD38 monoclonal antibodies that are specifically taken up by human MCL cells in the bone marrow of xenografted mice. When loaded with siRNAs against cyclin D1, CD38-targeted LNPs induced gene silencing in MCL cells and prolonged survival of tumor-bearing mice with no observed adverse effects. These results highlight the therapeutic potential of cyclin D1 therapy in MCL and present a novel RNAi delivery system that opens new therapeutic opportunities for treating MCL and other B-cell malignancies.

nanomedicine | siRNA | mantle cell lymphoma | cyclin D1 | CD38

RNA interference (RNAi) can be activated by introducing synthetic short double-stranded RNA fragments, termed small interfering RNAs (siRNAs), into cells to silence genes bearing complementary sequences. RNAi holds great promise as a powerful tool for evaluating the role of specific genes in cellular and disease processes and for therapeutic applications (1, 2). siRNAs that manipulate gene expression in leukocytes could be used to understand hematologic cell biology and to develop novel therapeutic approaches to dampen inflammation and the harmful immune responses that occur during autoimmunity; to suppress lymphotropic viral infections, such as HIV; or to treat blood cancers (3). However, the lack of systemic delivery startegies to target leukocytes foils these applications.

Here we devised a new strategy to target B-cell malignancies using mantle cell lymphoma (MCL) as a prototypic blood cancer to validate this siRNA delivery approach. MCL is an aggressive B-cell malignancy characterized by a $t(11:14)$ chromosomal translocation that juxtaposes the proto-oncogene encoding cyclin D1 (cycD1) to the Ig heavy chain gene promotor (4). This leads to constitutive overexpression of cycD1, a protein that is not expressed in healthy B-lymphocytes. Current MCL therapy relies mainly on conventional chemotherapy; anti-CD20 cytotoxic monoclonal antibodies; autologous stem cell transplantation; and, more recently, small molecule inhibitors of critical molecular pathways, such as the BTK inhibitor ibrutinib (5). Unfortunately, relapse and progressive resistance to treatment lead to short median survival. MCL has one of the worst prognoses among lymphomas (6–8). Thus, there is a need for new therapeutic approaches.

We previously showed that cycD1 down-regulation in MCL cell lines using RNAi inhibits proliferation and causes cell cycle arrest and apoptosis (9). However, the clinical application of this approach is hindered by the lack of appropriate systems that could deliver RNAi payloads to MCL cells in an efficient and safe manner (10, 11). RNAi therapeutics for B-cell malignancies is especially challenging because these cells are dispersed and are intrinsically resistant to transfection with nucleic acids (3, 12, 13). Therefore, to test the potential therapeutic effect of cycD1 inhibition in vivo and to demonstrate the feasibility of RNAi therapeutics in MCL, we needed to develop a suitable RNAi-delivery platform for potent gene silencing.

Lipid-based nanoparticles (LNPs), composed of ionizable lipids that incorporate siRNAs, can induce potent gene silencing in the liver (14, 15). These are currently being evaluated in a phase III clinical study to knock down the *TTR* gene expressed in the liver to treat familial amyloidosis (16). We recently demonstrated that LNPs could be surface-modified with a natural ligand or a monoclonal antibody to improve in vivo delivery of siRNA payloads (17, 18). Here we investigate the use of antibody-targeted LNPs to deliver siRNAs to MCL cells. The blood

Significance

RNA interference (RNAi) holds great promise as a novel therapeutic approach. Small interfering RNAs (siRNAs) that manipulate gene expression in leukocytes could be used to treat blood cancers. However, the lack of strategies for delivering siRNAs to leukocytes systemically has hampered the development of RNAi-based therapeutics. Here, we show that lipid-based nanoparticles coated with anti-CD38 monoclonal antibodies specifically target mantle cell lymphoma (MCL) cells and induce cell-specific therapeutic gene silencing in vivo. CD38-targeted nanoparticles that contain cyclin D1 siRNAs prolong survival of mice bearing MCL lymphomas in the bone marrow. This strategy opens a new avenue for treating MCL that might be applied to other hematological malignancies.

Author contributions: S.W., I.A.T., R.E., and D.P. designed research; S.W., I.A.T., R.E., S.R., I.H.-H., D.R., and M.G. performed research; A.A., O. Benjamini, O. Bairey, P.R., A.N., and J.L. contributed new reagents/analytic tools; S.W., I.A.T., and D.P. analyzed data; P.R. and A.N. provided clinical insight; and S.W., I.A.T., J.L., and D.P. wrote the paper.

Conflict of interest statement: J.L. is on the Scientific Advisory Board of Alnylam Pharmaceuticals. D.P. declares financial interests in Quiet Therapeutics. The rest of the authors declare no financial interest.

This article is a PNAS Direct Submission.

[1]S.W. and I.A.T. contributed equally to this work.

[2]To whom correspondence should be addressed. Email: peer@tauex.tau.ac.il.

This article contains supporting information online at www.pnas.org/lookup/suppl/doi:10.1073/pnas.1519273113/-/DCSupplemental.

supply in the hematological tissues where MCL cells mostly reside, including spleen and bone marrow, is made up of sinusoids that allow small nanoparticles tissue access. Selective targeting of lymphoma cells by antibody-targeted delivery should be clinically beneficial because it could reduce the total amount of drug required for therapeutic benefit and reduce toxicity to bystander cells (2, 12).

CD38 is expressed on the surface of immature hematopoietic cells, including immature B cells. Its expression is tightly regulated during B-cell ontogeny; it is expressed on bone marrow precursors, but not mature B cells. CD38 is expressed on most MCLs (19). In the present study, we show that CD38 is a suitable target for antibody-mediated delivery of therapeutic siRNAs to MCL. LNPs–siRNA coated with an anti-CD38 monoclonal antibody (αCD38 mAb) showed specific MCL binding in vitro (in MCL cell lines and MCL primary lymphomas) and in vivo (in mice xenografted with a human MCL cell line). CD38-targeted LNPs (αCD38-LNPs) entrapping siRNA against cycD1 (siCycD1) were specifically taken up by MCL xenografts. αCD38-LNPs-siCycD1 induced gene silencing, suppressed tumor cell growth in vitro, and prolonged the survival of MCL-bearing mice. Our data demonstrate the effectiveness of inhibiting cycD1 in MCL in vivo and highlight αCD38–LNPs–siRNA as part of a strategy that could ultimately become a novel therapeutic modality for treating MCL and other CD38-expressing hematological malignancies.

Results

MCL Cells Are Engrafted Mainly in the Bone Marrow of SCID Mice: Model Establishment. To test the ability of αCD38-LNPs-siCycD1 to target dispersed MCL cells, we first needed to establish an animal model of disseminated MCL in which MCL cells home to the bone marrow (BM), as in the advanced stages of the human disease. Granta-519 cells (2.5×10^6) stably expressing GFP (Granta-GFP) were injected i.v. into 6- to 8-wk-old female C-mB-17 SCID mice. These mice developed hind-leg paralysis after 24–30 d, at which time liver, lungs, spleen, kidney, blood, and BM cells were harvested to assess the distribution of MCL cells by flow cytometry. Granta-GFP cells consistently homed to the bone marrow (Fig. 1*A*). There were also some tumor cells in the lung, but very few in the liver, kidney, spleen, or blood. Bone marrow tumors that displaced normal bone marrow were prominent in H&E-stained femoral slices (Fig. 1*B*).

CD38: A Receptor Target for MCL. Targeting siRNAs selectively to tumors requires the identification of a cell-surface receptor that is overexpressed on tumor cells compared with most other tissues, the binding of which leads to endocytosis and release of endocytosed siRNAs into the target cell cytoplasm (2). Consistent with previous reports (19), we found that CD38 is highly and broadly expressed on four MCL lines that we tested (Fig. 2*A*) and on human primary MCL samples (Fig. 2*B*). In vitro incubation of Granta-519 cells with fluorescently labeled CD38 mAb (clone THB-7, αCD38) led to internalization of the antibody-receptor complex (Fig. 2*C*). Next, we looked at labeled αCD38 mAb binding after i.v. injection into mice bearing Granta-GFP lymphomas (Fig. 2*D*). Virtually all of the GFP+ lymphoma cells in the BM and lung bound the antibody. Although only few normal GFP− liver, blood, or lung cells bound αCD38, about half of GFP− spleen cells and a quarter of kidney cells bound it, but the staining was generally less intense than for the GFP+ tumor cells. These findings indicate the potential of THB-7 mAb and the CD38 receptor to serve as targeting moiety and target receptor, respectively, for specific delivery of LNPs to MCL in vivo.

Efficient Production of MCL-Targeted Lipid Nanoparticles Entrapping siRNAs. We next constructed LNPs encapsulating siRNAs using a microfluidic mixing system as previously described (17, 18, 20) (Fig. 3*A*). The lipid mixture contained the ionizable lipid Dlin-MC3-DMA

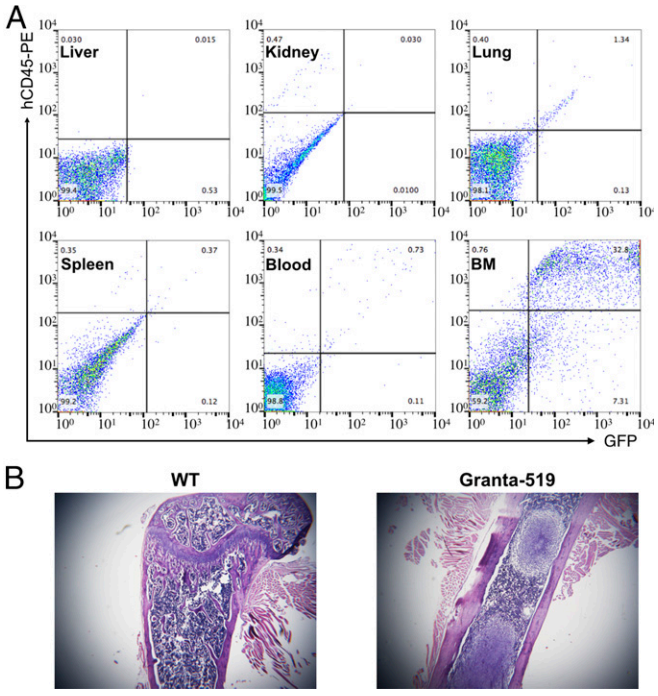

Fig. 1. MCL-xenograft model. Granta-GFP cells were i.v.-injected into CB-17 SCID mice. (*A*) Indicated organs were extracted when mice developed hind-leg paralysis. Single-cell suspensions were prepared and analyzed for Granta-GFP presence by flow cytometry (GFP+/hCD45+). (*B*) H&E stain on femur bones from untreated and MCL-bearing mice.

(14, 17) (50 mol %), cholesterol (38%), distearoyl phosphatidylcholine (DSPC, 10%), dimyristoyl polyethylene glycol (DMG-PEG, 1.95%), and distearoyl-phosphoethanolamine (DSPE)-PEG-maleimide (0.05%). αCD38 mAb (clone THB-7) was reduced to allow its chemical conjugation to maleimide groups present in the LNPs and then incubated with the LNPs. The αCD38–LNPs–siRNA had a mean diameter of ∼116 nm with a narrow size distribution [polydispersity index (PDI) ∼0.157] as measured by dynamic light scattering (DLS) (Table 1). ζ-Potential measurements showed a slight negative surface charge, as expected, at physiological pH (21). Transmission electron microscopy (TEM) analysis of the LNPs indicated a globular shape and size distribution in accordance with the DLS measurements (Fig. 3*B*).

αCD38–LNPs–siRNA Specifically Bind and Internalize into MCL Cells. To test whether αCD38–LNPs–siRNA specifically bind to MCL cells, we cocultured human MCL with CD38− mouse T lymphoma TK-1 cell lines and treated the mixtures with αCD38–LNPs–siRNA containing fluorescently labeled siRNAs (Fig. 3*C*). siRNA uptake was determined by flow cytometry. αCD38–LNPs–siRNA selectively bound to the MCL cell lines, as indicated by higher fluorescence intensity levels in those cells. Moreover, addition of free unlabeled αCD38 mAbs to the cocultures decreased particle binding to background levels, indicating that binding was via CD38. We obtained similar results using two primary human MCL samples (Fig. 3*D*). Next we incubated Granta-519 cells with LNPs that were uncoated or coated with αCD38 or an isotype control antibody and entrapped fluorescently labeled siRNAs. Following incubation, we imaged the cells by confocal microscopy using αCD20 to stain their cell surface (Fig. 3*E*). Bound and internalized siRNA was detected only with the αCD38-coated LNPs.

αCD38-LNPs-siCycD1 Induce Robust Gene Knockdown and Cell Cycle Arrest. Next we examined whether αCD38-LNPs loaded with

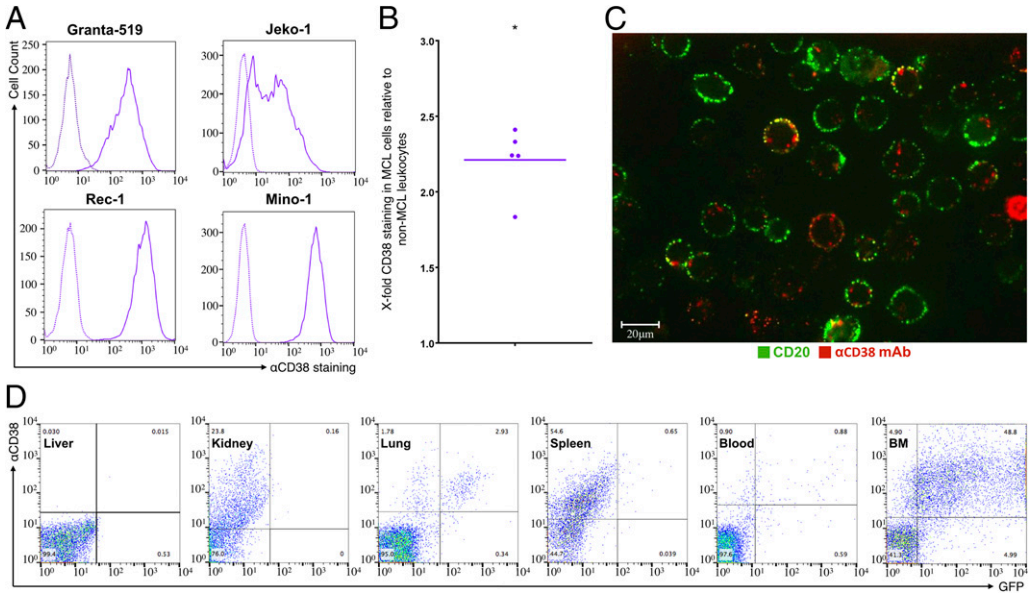

Fig. 2. αCD38mAb targets MCL cells and induces cellular internalization. (*A*) αCD38 mAb binding to four MCL cell lines. Continuous line: αCD38. Dashed lines: isotype control. (*B*) αCD38 mAb binding to MCL cells (CD5+/CD19+) relative to non-MCL leukocytes present in blood samples from MCL patients. Each dot represents one sample ($n = 5$); horizontal bar represents mean (*$P < 0.05$; two-tailed Student's t test for paired values). (*C*) αCD38 mAb internalization upon binding to Granta-519 cells. (Scale bar: 20 μm.) (*D*) In vivo binding of αCD38 mAb to different organs in representative MCL-bearing mouse. Indicated organs were extracted 2 h post αCD38 mAb injection, suspended, and analyzed by flow cytometry. αCD38 mAb can be found on most MCL cells (Granta-GFP cells) in the BM.

cycD1 siRNA (siCycD1), or as control luciferase siRNA (siLuc), could mediate gene silencing in two MCL cell lines, Granta-519 and Jeko-1 (Fig. 3 *F* and *G*). When these MCL cell lines were treated with αCD38-LNPs-siCycD1, they had in average 55.7% ($P < 0.001$) and 56% ($P < 0.002$) reduction in CycD1 protein levels as determined by flow cytometry compared with αCD38-LNPs-siLuc. The latter particles did not significantly affect CycD1 levels. CycD1 knockdown was also confirmed at the mRNA level by qRT-PCR (Fig. S1). As expected (9), the reduction in CycD1 levels in the αCD38-LNPs-siCycD1–incubated cells caused a cell cycle arrest in the G_0/G_1 phase (Fig. 3*H*). This effect was evident even though down-regulation of cycD1 induced compensatory elevation of other D-cyclin expression (Fig. S2).

αCD38-Coated LNPs Specifically Target MCL Cells in Vivo. Next, we tested the ability of αCD38–LNPs–siRNA to deliver siRNAs into Granta-519 xenografts in vivo. When hind-leg paralysis appeared, MCL-bearing mice were mock-treated or treated i.v. with LNPs and loaded with fluorescently labeled siRNAs, which were coated with αCD38 or an isotype control antibody. BM was extracted 2 h later and analyzed by flow cytometry for siRNA uptake into mouse CD45+ cells and the human tumor, stained with anti-human CD20 antibody (Fig. 4 *A* and *B*). Fluorescent siRNAs were detected in ∼30% of MCL cells in mice treated with αCD38–LNPs–siRNA, compared with ∼6% of isotype-LNPs–siRNA ($P < 0.0002$). Although about 15% of mouse BM cells were labeled with the fluorescent siRNA, there was no significant difference in siRNA accumulation between mice treated with αCD38 or control antibody-coated LNPs ($P = 0.38$). Thus, αCD38–LNPs–siRNA specifically bind to MCL cells in the BM in vivo.

CD38-LNPs-siCycD1 Induce Therapeutic Gene Silencing in MCL Cells in Vivo. We next examined the therapeutic effect of CD38-LNPs-siCycD1 on the survival of MCL-bearing mice. Mice ($n = 10$/group) were treated biweekly with 9 i.v. injections of 1 mg/kg siRNA, starting 5 d after tumor inoculation. Control mice were mock-treated or treated with CD38-LNPs-siLuc. No loss in body weight was observed during the first 21 d of the experiment, indicating that the treatments did not induce major adverse effects (Fig. S3). Treatment with αCD38-LNPs-siCycD1 increased median survival from 34 to 49 d ($P = 0.0087$) compared with αCD38-LNPs-siLuc treatment (Fig. 4*C*). Survival of mice treated with the luc-targeting control LNPs was not significantly different from survival of mock-treated mice. These findings represent, to our knowledge, the first indication of the therapeutic benefit of using siCycD1 in vivo in MCL-bearing mice.

Discussion

The discovery of RNAi in human cells raised the possibility of suppressing expression of any disease-causing gene and suggested a highly promising strategy for personalized medicine to treat cancer and other diseases. However, the efficient, specific and safe delivery of RNAi payloads remains a major challenge facing the application of RNAi therapeutics to most diseases (2, 11). The use of RNAi for treating B-cell lymphomas has been stymied by the lack of an appropriate delivery system. The methods that work in vitro (such as electroporation) are not suitable for systemic in vivo application, whereas others (such as viral vectors) raise safety issues (22, 23). Here, we report that siRNAs against cycD1 prolonged the survival of mice bearing a human MCL cell line xenograft. In vivo gene knockdown was possible with systemic administration of siRNAs entrapped in newly developed and characterized lipid-based nanoparticles coated with THB-7 monoclonal antibodies targeting the CD38 cell marker. The αCD38-LNPs-siCycD1 specifically bound to MCL cells and induced protection in vivo and in tissue culture and therefore constitute a potent RNAi delivery system for MCL. This delivery system has an encouraging initial safety profile because repeated systemic administration did not affect body weight. In prior studies, performed in nonhuman primates and currently under phase III clinical trials, the LNP components that we used (except for the uninvestigated mAbs) showed satisfactory biocompatibility and little or no immune response (11, 14, 16–18, 24). However, more extensive toxicity studies are needed.

These LNPs were produced by a scalable production process that increases siRNA encapsulation and transfection potency

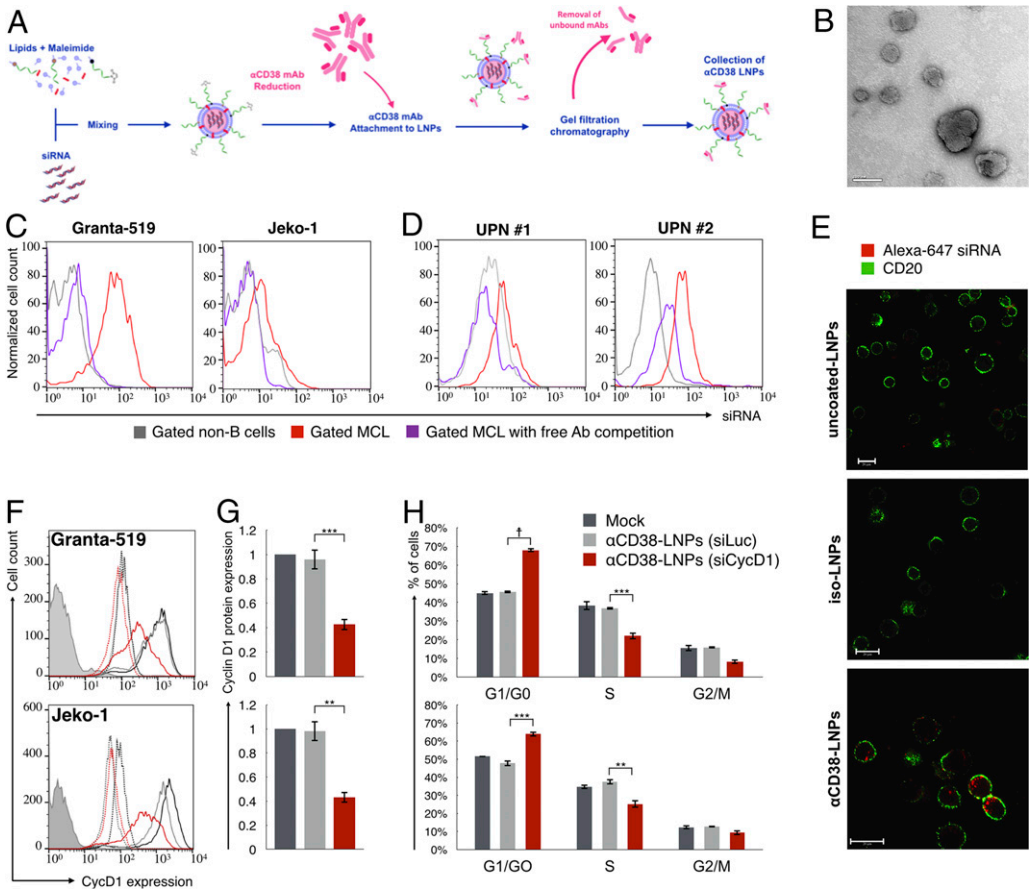

Fig. 3. αCD38–LNPs–siRNA mediate active delivery of siRNA specifically into MCL cells and induce antitumor gene silencing. (*A*) Schematic diagram of the αCD38–LNPs–siRNA production process. (*B*) Transmission electron microscopy image of αCD38–LNPs–siRNA. (Scale bar: 100 nm.) (*C*) Granta-GFP (*Left*) or Jeko-GFP (*Right*) were cocultured with TK-1 (murine T-lymphoma) cells and incubated with αCD38–LNPs–siRNA entrapping labeled siRNA. (*D*) Mononuclear cells from two blood samples of MCL patients were incubated with αCD38–LNPs–siRNA including labeled siRNA. *C* and *D* exhibit siRNA-LNPs binding to non-B cells (gray), MCL cells (red), or MCL cells in samples incubated with free competing αCD38 mAbs before αCD38–LNPs–siRNA incubation (purple). (*E*) Granta-519 cells uptake of siRNA delivered via indicated LNPs and visualized by live confocal microscopy. (Scale bar: 20 μm.) (*F* and *G*) Granta-519 (*Upper*) or Jeko-1 (*Lower*) were incubated with mock (black), αCD38-LNPs-siLuc (gray), or αCD38-LNPs-siCycD1 (red). Forty-eight hours post treatment, cells were analyzed for cycD1 protein expression by flow cytometry. (*F*) Representative data from one of five (Granta) or three (Jeko) experiments. Continuous lines: cycD1 staining. Dashed lines: isotype control. Filled histogram: unstained. Complete data are represented in *G*. Bar plots represent mean ± SEM of cycD1 expression normalized to mock (**$P < 0.01$; ***$P < 0.001$; one-way ANOVA test with Bonferroni correction). (*H*) Cell cycle distribution of cells 48 h post treatments with mock (black), αCD38-LNPs-siLuc (gray), or αCD38-LNPs-siCycD1 (red) analyzed by flow cytometry. Bars represent mean percentage ± SEM of $n = 4$ from two independent experiments per cell line (**$P < 0.01$; ***$P < 0.001$; †$P < 10^{-4}$; one-way ANOVA test with Bonferroni correction).

(20). Similar LNPs demonstrated potent siRNA activity in hepatocytes (14), which are relatively easy to transfect in vivo. However, MCL cells, like other lymphomas and most hematopoietic cells, are dispersed throughout the body and are not easily transfected by LNPs or conventional lipid-based transfection reagents. Therefore, a practical siRNA-targeted platform for lymphomas was needed. We previously showed that in vivo gene knockdown in lymphocytes could be achieved using anti-integrin antibody fragments that were engineered as fusion proteins with protamine that bound to siRNAs or antibody-derivatized LNPs that encapsulated siRNAs (25, 26). These proof-of-concept studies are, to our knowledge, the first to show systemic delivery of siRNAs into lymphocytes. However, these studies used a delivery approach, which is not scalable, and an mAb targeting an integrin molecule that is expressed on all leukocytes and lack selectivity to subsets of cells.

To achieve specificity for targeting MCL cells, the LNPs were coated with an anti-CD38 mAb (clone THB-7). This mAb recognizes the surface protein CD38, which is found on immature leukocyte precursors but overexpressed in MCL tumor cells and other B-cell hematological malignancies, such as in chronic lymphocytic leukemia (where it correlates with poor prognosis) and multiple myeloma (27–29). In MCL, elevated expression of CD38 is correlated with adhesion to stromal cells in lymphoid tissues, a niche considered to be favorable for tumor proliferation (19). MCL tumors resistant to bortezomib, a proteasome inhibitor approved for relapsed MCL, show increased CD38 levels, emphasizing a potential advantage of targeting CD38 (30). In this study, the THB-7 αCD38 mAbs were used as a MCL-targeting moiety and did not display significant antitumor activity by

Table 1. Characterization of αCD38–LNPs–siRNA by dynamic light scattering and ζ-potential measurements

Examined characteristic	Mean ± SD
Hydrodynamic diameter	116 ± 7.9 nm
Polydispersity index	0.157 ± 0.017
ζ-Potential	−5.83 ± 1.1 mV

Data are represented as mean ± SD of 12 (size and PDI) or 2 (ζ-potential) measurements for independently produced batches. All individual measurements included three technical replicates.

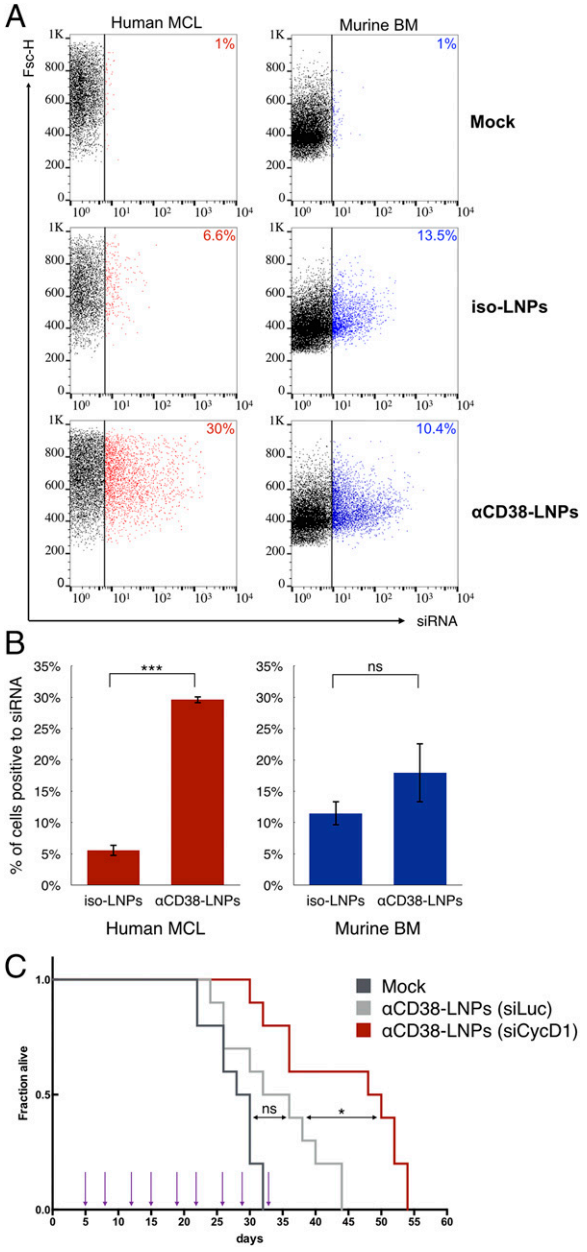

Fig. 4. αCD38-LNPs-siCycD1 target MCL xenografts in the BM and prolong the survival of diseased mice. (*A* and *B*) Mice bearing human MCL cells were i.v.-injected with mock, isotype-, or αCD38–LNPs–siRNAs. Bone marrow cells were extracted 2 h later and analyzed for LNP binding as detected by siRNA fluorescence via flow cytometry. Human MCL (*Left*) and murine (*Right*) cells were gated separately based on GFP, hCD20, and mCD45 expression. Cells with siRNA fluorescence levels higher than in the top 1% of cells from mock-treated mice were considered positive (siRNA-positive cells are colored; cutoff is represented by the vertical bar). (*A*) Dot plots for one representative animal from each treatment group (isotype: $n = 2$; αCD38: $n = 3$). Number indicates percentage of siRNA-positive cells. Complete results are shown in *B*. Bar plots represent mean ± SEM (ns $P > 0.05$; ***$P < 0.001$; two-tailed Student's *t* test). (*C*) Survival curves of MCL-bearing mice. Corresponding treatments (1 mg siRNA/kg body) were administrated at nine time points (arrows) via retro-orbital route. $n = 10$ animals per group. *P* values and significance were determined by log-rank Mantel–Cox test with Bonferroni correction (*$P < 0.05$).

themselves (Figs. 3*H* and 4*C*, siLuc). Nevertheless, because THB-7 binding induced endocytosis in MCL cells, this mAb could mediate active delivery of siRNAs into the cytoplasm of targeted cells. Further investigations will be needed to assess whether αCD38–LNPs–siRNA are internalized and induce gene silencing in other CD38-implicated diseases.

Currently, anti-CD38 antibodies are examined in clinical trials and demonstrate promising antitumor effects in multiple myeloma (31, 32). The lack of antitumor effect by the mAb itself in this present work could be attributed to the use of different antibody clone (THB-7). This explanation is supported by the fact that the THB-7 clone was previously shown to be less effective in inhibition of myeloid cell growth than other anti-CD38 clones (33). It could be interesting to further use the promising anti-CD38 clones tested in those clinical trials in our LNP formulation and examine whether they could lead to a greater antitumor effect due to synergitic actions of the siRNA and mAB. Moreover, because the LNP therapeutic strategy is modular, it is possible to use different antibodies as targeting moieties for MCL cells and other B-cell malignancies (including those that do not express the CD38 protein). However, it is essential to take into account that changing the targeting moeity warrants testing the strategy in appropriate cell types and animal models. The matching of the appropriate targeting moiety to the surface receptor expressed on the target cells needs to be carefully examined as some receptors might cluster on the cell surface and induce an outside-in signaling event that could lead to proliferation.

MCL cells, like other B cells, are highly resistant to transfection (34). Nevertheless, the gene silencing that we obtained with the αCD38-LNPs-siCycD1 in vitro was potent, highlighting the potential of the αCD38-LNPs to serve as a powerful RNAi tool not only for therapeutic applications, but also as a research tool for using in vivo gene knockdown to study B-cell biology. In the in vivo studies, we did not succeed in demonstrating gene silencing in a direct manner. However, former studies performed in vitro demonstrated that the silencing of cycD1 induces cell cycle arrest and cell death (9). These findings imply there should be a "selective force" against the targeted cells in which cycD1 was knocked down, interfering with the ability to detect the silencing of cycD1 in the BM of tumor-bearing mice. To overcome this problem, we decided to investigate the ability of the treatments to display an overall survival benefit. We conclude that the prolonged survival of the mice treated with the αCD38-LNPs-siCycD1, relative to the survival of the mice treated with αCD38-LNPs-siLuc and mock-treated mice, must be attributed to the effect of cycD1 silencing.

CycD1 overexpression is a prominent genetic hallmark and tumorigenic factor in MCL. The relevance of selective cycD1 silencing in MCL has been questioned before due to compensatory elevation of cyclin D2 expression (35, 36). In accordance with precedent reports, we detected that the down-regulation of cycD1 expression induces a compensatory up-regulation of cyclin D2 expression (Fig. S2). We detected a similar compensatory expression pattern regarding cyclin D3 as well. The compensatory expression of these genes did not mask the effects of cycD1 silencing in MCL cells (demonstrated in ref. 9 and in Fig. 3 *G* and *H*). Still, previous studies have shown that the compensatory activity of other D cyclins allows cycD1 knockout mice to be viable and to show only limited developmental defects (37). Therefore, it is reasonable to argue that undesired nonspecific uptake of αCD38-LNPs-siCycD1 by non-MCL bystander cells would be expected to exhibit only low or no adverse effects.

In addition to cycD1, the repertoire of potential RNAi targets for MCL therapy is constantly growing by virtue of the expanding knowledge of molecular mechanisms involved in the disease's pathogenesis (4). Moreover, the advances in sequencing technologies allow access to the transcriptome of individual tumors and thus would certainly highlight new targets in a personalized resolution. Thanks to its easily scalable production process and its compatibility with any siRNA sequence as well as a wider range of RNAi molecules, the αCD38–LNPs–siRNA platform arises as an appropriate carrier for the testing and validation of therapeutic

gene silencing and potentially as a powerful tool in the service of precision medicine for the treatment of B-cell malignancies.

Materials and Methods

Materials. All lipids used for LNP production were purchased from Avanti Polar lipids except for Dlin-MC3-DMA, which was synthesized in our laboratory according to a reported method (14). siRNA molecules were designed and screened by Alnylam Pharmaceuticals. The following sequences (sense strand) were used: siCycD1—GUAGGACUCUCAUUCGGGATT; siLuc—CUUACGCUGAGUACUUCGATT. Alexa-647–labeled siRNA possessed the same sequence as siLuc. The monoclonal antibodies THB-7 (mouse IgG1 anti-hCD38) and MOPC-21 (mouse IgG1 isotype ctrl) were purchased from BioXcell. Granta-519 and Jeko-1 cells were purchased from DSMZ, and TK-1, Mino, and Rec-1 cells were purchased from the American Type Culture Collection and cultured as recommended by the providers.

Production of Targeted LNPs. LNPs–siRNA were prepared by microfluidic micro mixture (Precision NanoSystems). One volume of mixed lipids (Dlin-MC3-DMA, cholesterol, DSPC, DMG-PEG, and DSPE-PEG-maleimide at a 50:38:10:1.95:0.05 molar ratio, 9.64 nM total lipid concentration) in pure ethanol and 3 vol of siRNA (1:16 wt/wt siRNA to lipid) in an acetate buffer solution were injected into the micromixer in a controlled flow rate (0.5 mL/min for ethanol and 1.5 mL/min for aqueous buffer). For labeled LNPs, 10% of Alexa-647–labeled siRNA were incorporated. The resultant mixture was dialyzed overnight against PBS (pH 7.4) to remove ethanol. THB-7 or isotype mAbs (MOPC-21) were reduced with DTT (1 and 5 mM, respectively) for 30 min shaking in 37 °C. DTT was removed with 7-k Zeba spin desalting columns (Thermo) according to the manufacturer's protocol. The thiolized mAbs were incubated with the LNPs for 2 h in gentle shaking at room temperature. Removal of unconjugated mAbs was performed by loading the LNPs on gel filtration chromatography columns containing Sepharose CL-6B beads (Sigma-Aldrich) with PBS as a mobile phase. The bead column was washed with 0.1 M NaOH and readjusted with PBS before sample loading. The mAbs-LNPs–siRNA were reconcentrated via 100 k Amicons Ultra-4 (Millipore) and filtered through a 0.2-μm membrane (Sartorius).

Size, ζ-Potential, and Ultrastructure Analysis of αCD38–LNPs–siRNA. LNP size distribution and ζ-potential were determined by dynamic light scattering using a Malvern nano ZS ζ-sizer (Malvern Instruments). For size measurements, LNPs were diluted 1:20 in PBS. All used samples showed a PDI lower than 0.2. For ζ-potential measurements, LNPs were diluted 1:200 in double-distilled water. Size and shape of LNPs were analyzed by TEM. LNPs in PBS were placed on a formvar/carbon-coated copper grid, air-dried, and stained with 2% (wt/vol) aqueous uranyl acetate. The analysis was performed with a Philips Tecnai F20 field emission TEM operated at 200 kV.

In Vitro Binding Experiments. THB-7 (αCD38) mAb was labeled with an Alexa Fluor(R) 647 protein-labeling kit (Invitrogen). Binding of the labeled mAb to MCL cell lines was assessed by flow cytometry (BD FACScalibur, with CellQuest software for data collection and FlowJo software for data analysis). To determine the specific binding of αCD38–LNPs–siRNA, MCL cell lines expressing GFP and the murine T-lymphoma TK1 cell line (0.5×10^6 each) were incubated together on ice with either 1% FCS PBS or with the buffer including 1 μg of free αCD38 mAb. After 15 min, αCD38–LNPs–siRNA with labeled siRNA were added (0.5 μg total siRNA) for an 30 additional minutes. Cells were collected for flow cytometry analysis after three rounds of PBS wash. Cell populations were separately gated based on GFP fluorescence.

In Vitro Internalization Experiments. Granta cells (0.5×10^6) were incubated in 50 μL of 1% serum PBS at 4° with Alexa-647 αCD38 or isotype control mAbs for 10 min and then incubated for 2 h at 37 °C (5% CO_2). Then cells were washed twice, stained with PE-hCD20 mAbs (Biolegend, 302306) for 30 min on ice, washed, and subjected to confocal microscopy analysis. For assessing the internalization of αCD38–LNPs–siRNA, 0.5×10^6 Granta cells were incubated in 50 μL of 1% serum PBS on ice with αCD38-, isotype-, or uncoated siRNA-LNPs including labeled siRNA (500 ng of total siRNA). After 10 min, cells passed through three rounds of PBS wash and were reincubated in fresh medium for 4 h at 37 °C (5% CO_2). Then cells were washed, stained with PE-hCD20 mAbs for 30 min on ice, washed, and subjected to confocal microscopy analysis. All pictures were obtained on live cells using the Nikon Eclipse C2 configured with NI-E microscope and processed with NIS-elements software using ×40 objective magnification (Nikon).

In Vitro Gene Silencing. Granta-519 or Jeko-1 cells (0.3×10^6) were placed in tissue culture 24-well plates with 0.5 mL of full medium. αCD38-LNPs-siCycD1 or αCD38-LNPs-siLuc were added to the wells (2 μg of siRNA for each condition). After 18 h of incubation under standard culture conditions, cells were washed three times and reincubated in fresh medium under culture conditions. Forty-eight hours following initial exposure to treatments, cells were collected for cycD1 protein quantification, mRNA quantification, or cell cycle measuring. cycD1 intracellular staining was performed according to the BD Pharmingen Transcription Factor Buffer set instructions using rabbit anti-human cycD1 monoclonal antibody (Cell Marque, 241R-16) or isotype control (Jackson ImmunoResearch, 011–000-003) at 0.68 μg/mL. Cells were washed and incubated with 2 μg/mL of Alexa647 donkey anti-rabbit antibody (Jackson ImmunoResearch, 711–605-152) for 30 min at 4 °C, washed twice, and analyzed by flow cytometry. The geometric mean of detected Alexa Fluor-647 fluorescence intensity for at least 5,000 cells was used as the compared value for each sample. cycD1 relative expression for each treatment group was derived from the quotient of the value of cycD1 staining divided by the value of isotype ctrl staining.

Cell Cycle Studies. The transfected cells were washed with ice-cold PBS and fixed with 70% ethanol for 1 h. Then the cells were washed twice with cold PBS and incubated for 10 min at 37 °C in 250 μL PBS with 10 μg/mL propidium iodide (PI), 2.5 μg/mL DNase-free RNase A (Sigma), and 0.01% Triton-X. PI fluorescence was assessed by flow cytometry. Analyses by FlowJo were performed on at least 9,000 cells per sample after gating out debris and cell duplets based on the FL2-Area/FL2-Width channels. Cell cycle distributions were obtained via the application of the Dean–Jett–Fox model on gated cells with root mean square scores ranging between 1.5 and 2.5.

Ex Vivo Binding with Human MCL Primary Samples. Peripheral blood samples were obtained from MCL patients treated at the Rabin Medical Center (Petah Tikva) and the Chaim Sheba Medical Center at Tel Hashomer (Ramat Gan) in accordance with institutional review board-approved informed consent. Mononuclear cells were extracted from full blood samples using Ficoll-Paque PLUS (GE Healthcare). Cells (1×10^6) from the primary sample were incubated with targeted LNPs and free competing αCD38 mAb as described in the in vitro binding experiments. After three rounds of wash, cells were stained with CD19 (Biolegend, 302219) and CD45 (Biolegend, 304008) mAbs for 30 min on ice. Membranal staining was used during analysis to separate B-lymphocytes (CD19+/CD45+) from non-B leukocytes populations (CD19–/CD45+) while assessing for siRNA fluorescence.

Human MCL Xenograft Mouse Model. To enable easier identification of the MCL cells in vivo, Granta-519 cells were stably infected with pTurbo-GFP retroviral particles (kindly supplied by Eran Bacharach, Department of Cell Research and Immunology, George S. Wise Faculty of Life Sciences, Tel Aviv University, Tel Aviv, Israel). The infected cells were sorted according to their GFP expression, and the highest GFP population (Granta-GFP) was collected and grew.

For modeling MCL in vivo, female C.B-17/IcrHsd-Prkdcscid mice were purchased from Harlan Laboratories. The mice were housed and maintained in laminar flow cabinets under specific pathogen-free conditions in the animal quarters of Tel Aviv University and in accordance with current regulations and standards of the Israel Ministry of Health. All animal protocols were approved by Tel Aviv University Institutional Animal Care and Use Committee.

Granta-519 or Granta-GFP cells (2.5×10^6) were i.v.-injected into 8-wk-old mice. Mice were monitored daily and killed when disease symptoms appeared (15% reduction in body weight or hind-leg paralysis). Different tissues and organs (liver, kidney, lungs, spleen, blood, bone marrow, and if existing, solid tumor) were collected with respect to the different experiments and processed into single-cell suspensions. To identify the MCL cells, cell suspensions were analyzed by flow cytometry, using PE mouse anti-human CD45 antibody, PE, or Alexa 647 mouse anti-human CD20 (Biolegend, 302318) antibodies and/or GFP expression. Femour bones were fixed, sliced, decalcified, and stained with H&E as described before (38).

In Vivo Binding of αCD38 mAb. MCL xenograft mice were i.v.-injected with 30 μg of Alexa-647–labeled αCD38 or isotype control mAbs at day of hind-leg paralysis appearance. Two hours later, mice were scarified, and liver, kidneys, lungs, spleen, and bone marrow were harvested and processed into single-cell suspensions. αCD38 fluorescence on cells was assessed by flow cytometry.

In Vivo Binding of Targeted LNPs. At day 24 post tumor injection, saline, isotype-, or αCD38-LNPs-siCycD1 including labeled siRNA (1.25 mg siRNA/kg body) were administered i.v. via the tail vein. After 2 h, mice were killed, and cells from the bone marrow were extracted. Single-cell suspensions were prepared by passing the cells through 70-μm cell strainers (BD) and washing with PBS. Cells were stained with Alexa Fluor-488-hCD20 (Biolegend, 302316) and PE-mCD45 (Biolegend 103106) mAbs for 30 min and washed before analysis. Human MCL cells (GFP+/hCD20+/mCD45–) and murine cells (GFP–/hCD20–/mCD45+) were gated separately and assessed for siRNA fluorescence. The cells from the mock-treated mouse were used as a baseline for negative fluorescence, whereas cells in other groups were considered positive to siRNA fluorescence if exhibiting higher values than the 99th percentile's value of mock-treated mice.

Survival Experiment. The survival experiment was performed at Charles Rivers Laboratories in accordance with the Association for Assessment and Accreditation of Laboratory Animal Care committee. Thirty MCL xenograft mice were divided into three treatment groups: untreated (mock), αCD38-LNPs-siLuc, and αCD38-LNPs-siCycD1. The different treatments (1 mg siRNA/kg body) were injected via retro-orbital route nine times (days 5, 8, 12, 15, 19, 22, 26, 29, and 33). Mice displaying loss of 15% body weight or limb paralysis were euthanized.

Statistical Analysis. In experiments with multiple groups, we used one-way ANOVA with Bonferroni correction. For the comparison of two experimental groups, we used the two-tailed Student's *t* test. A value of $P < 0.05$ was considered statistically significant. Analyses were performed with Prism 6 (Graphpad Software).

ACKNOWLEDGMENTS. We thank Dr. Leonid Mittelman and Dr. Vered Holdengreber for scientific assistance with confocal and electron microscopy and Andrew G. Sprague (Alnylam Pharmaceuticals) for providing siRNA and fluorescently labeled siRNA molecules. This work was supported in part by grants from the NIH (5R01CA139444-10); The Dotan Hematology Center at Tel Aviv University; The Lewis Family Trust; the Israel Science Foundation (Award #181/10); the I-CORE Program of the Planning and Budgeting Committee and The Israel Science Foundation (Grant 41/11) and the FTA: Nanomedicines for Personalized Theranostics of the Israeli National Nanotechnology Initiative; and by The Leona M. and Harry B. Helmsley Nanotechnology Research Fund (D.P.).

1. Behlke MA (2006) Progress towards in vivo use of siRNAs. *Mol Ther* 13(4):644–670.
2. Peer D, Lieberman J (2011) Special delivery: Targeted therapy with small RNAs. *Gene Ther* 18(12):1127–1133.
3. Peer D (2013) A daunting task: Manipulating leukocyte function with RNAi. *Immunol Rev* 253(1):185–197.
4. Jares P, Colomer D, Campo E (2012) Molecular pathogenesis of mantle cell lymphoma. *J Clin Invest* 122(10):3416–3423.
5. Wang ML, et al. (2013) Targeting BTK with ibrutinib in relapsed or refractory mantle-cell lymphoma. *N Engl J Med* 369(6):507–516.
6. Campo E, Rule S (2015) Mantle cell lymphoma: Evolving management strategies. *Blood* 125(1):48–55.
7. Cheah CY, et al. (2015) Patients with mantle cell lymphoma failing ibrutinib are unlikely to respond to salvage chemotherapy and have poor outcomes. *Ann Oncol* 26(6): 1175–1179.
8. Dreyling M; European Mantle Cell Lymphoma Network (2014) Mantle cell lymphoma: Biology, clinical presentation, and therapeutic approaches. *Am Soc Clin Oncol Educ Book* 2014:191–198.
9. Weinstein S, et al. (2012) RNA inhibition highlights cyclin D1 as a potential therapeutic target for mantle cell lymphoma. *PLoS One* 7(8):e43343.
10. Peer D (2014) Harnessing RNAi nanomedicine for precision therapy. *Mol Cell Ther* 2:5.
11. Wittrup A, Lieberman J (2015) Knocking down disease: A progress report on siRNA therapeutics. *Nat Rev Genet* 16(9):543–552.
12. Weinstein S, Peer D (2010) RNAi nanomedicines: Challenges and opportunities within the immune system. *Nanotechnology* 21(23):232001.
13. He W, et al. (2014) Discovery of siRNA lipid nanoparticles to transfect suspension leukemia cells and provide in vivo delivery capability. *Mol Ther* 22(2):359–370.
14. Jayaraman M, et al. (2012) Maximizing the potency of siRNA lipid nanoparticles for hepatic gene silencing in vivo. *Angew Chem Int Ed Engl* 51(34):8529–8533.
15. Tam YY, Chen S, Cullis PR (2013) Advances in lipid nanoparticles for siRNA delivery. *Pharmaceutics* 5(3):498–507.
16. Zimmermann T, et al. (2013) Phase I first-in-humans trial of ALN-TTRsc, a novel RNA interference therapeutic for the treatment of familial amyloidotic cardiomyopathy (FAC). *J Card Fail* 19(8):S66.
17. Cohen ZR, et al. (2015) Localized RNAi therapeutics of chemoresistant grade IV glioma using hyaluronan-grafted lipid-based nanoparticles. *ACS Nano* 9(2):1581–1591.
18. Ramishetti S, et al. (2015) Systemic gene silencing in primary T lymphocytes using targeted lipid nanoparticles. *ACS Nano* 9(7):6706–6716.
19. Chang BY, et al. (2013) Egress of CD19(+)CD5(+) cells into peripheral blood following treatment with the Bruton tyrosine kinase inhibitor ibrutinib in mantle cell lymphoma patients. *Blood* 122(14):2412–2424.
20. Belliveau NM, et al. (2012) Microfluidic synthesis of highly potent limit-size lipid nanoparticles for in vivo delivery of siRNA. *Mol Ther Nucleic Acids* 1:e37.
21. Leung AK, Tam YY, Cullis PR (2014) Lipid nanoparticles for short interfering RNA delivery. *Adv Genet* 88:71–110.
22. Peer D, Zhu P, Carman CV, Lieberman J, Shimaoka M (2007) Selective gene silencing in activated leukocytes by targeting siRNAs to the integrin lymphocyte function-associated antigen-1. *Proc Natl Acad Sci USA* 104(10):4095–4100.
23. Yin H, et al. (2014) Non-viral vectors for gene-based therapy. *Nat Rev Genet* 15(8): 541–555.
24. Novobrantseva TI, et al. (2012) Systemic RNAi-mediated gene silencing in nonhuman primate and rodent myeloid cells. *Mol Ther Nucleic Acids* 1:e4.
25. Peer D, Park EJ, Morishita Y, Carman CV, Shimaoka M (2008) Systemic leukocyte-directed siRNA delivery revealing cyclin D1 as an anti-inflammatory target. *Science* 319(5863):627–630.
26. Kim SS, et al. (2010) RNAi-mediated CCR5 silencing by LFA-1-targeted nanoparticles prevents HIV infection in BLT mice. *Mol Ther* 18(2):370–376.
27. Deckert J, et al. (2014) SAR650984, a novel humanized CD38-targeting antibody, demonstrates potent antitumor activity in models of multiple myeloma and other CD38+ hematologic malignancies. *Clin Cancer Res* 20(17):4574–4583.
28. Ibrahim S, et al. (2001) CD38 expression as an important prognostic factor in B-cell chronic lymphocytic leukemia. *Blood* 98(1):181–186.
29. Vaisitti T, et al. (2015) The enzymatic activities of CD38 enhance CLL growth and trafficking: Implications for therapeutic targeting. *Leukemia* 29(2):356–368.
30. Pérez-Galán P, et al. (2011) Bortezomib resistance in mantle cell lymphoma is associated with plasmacytic differentiation. *Blood* 117(2):542–552.
31. Wong SW, Comenzo RL (2015) CD38 monoclonal antibody therapies for multiple myeloma. *Clin Lymphoma Myeloma Leuk* 15(11):635–645.
32. Phipps C, Chen Y, Gopalakrishnan S, Tan D (2015) Daratumumab and its potential in the treatment of multiple myeloma: Overview of the preclinical and clinical development. *Ther Adv Hematol* 6(3):120–127.
33. Todisco E, et al. (2000) CD38 ligation inhibits normal and leukemic myelopoiesis. *Blood* 95(2):535–542.
34. Buschle M, et al. (1990) Transfection and gene expression in normal and malignant primary B lymphocytes. *J Immunol Methods* 133(1):77–85.
35. Klier M, et al. (2008) Specific lentiviral shRNA-mediated knockdown of cyclin D1 in mantle cell lymphoma has minimal effects on cell survival and reveals a regulatory circuit with cyclin D2. *Leukemia* 22(11):2097–2105.
36. Tchakarska G, Le Lan-Leguen A, Roth L, Sola B (2009) The targeting of the sole cyclin D1 is not adequate for mantle cell lymphoma and myeloma therapies. *Haematologica* 94(12):1781–1782.
37. Sherr CJ, Roberts JM (2004) Living with or without cyclins and cyclin-dependent kinases. *Genes Dev* 18(22):2699–2711.
38. Naresh KN, et al. (2006) Optimal processing of bone marrow trephine biopsy: The Hammersmith Protocol. *J Clin Pathol* 59(9):903–911.

Supporting Information

Weinstein et al. 10.1073/pnas.1519273113

SI Materials and Methods

Electroporation. One nanomole of each the siRNA duplexes (siLuc or siCycD1) was electroporated into 10×10^6 Granta-519 or Jeko-1 cells using the Amaxa 4D-nuclefactor system (CM-119 program, SF solution).

Quantitative Real-Time PCR. Total RNA was isolated using an EZ-RNA kit (Biological Industries), and cDNA was generated with a qScript cDNA Synthesis Kit (Quanta) according to the manufacturer's instructions. qRT-PCR was performed with Fast SYBR Green Master Mix and the ABI StepOnePlusTM instrument (Life Technologies). Expression of cyclins was normalized to the two "house-keeping" genes, *eIF3a* and *eIF3c*, using the multiple endogenous controls option. This option allows the software to treat all endogenous controls as a single population and calculates the experiment-appropriate mean to establish a single value against which the target of interest is normalized. The primers used for amplification are the following (5′–3′): CCND1 F—GAGGAGCCCCAACAACTTCC and R—GTCCGGGTCACACTTGATCAC; CCND2 F—CGCAAGCATGCTCAGACCTT and R—TGCGATCATCGACGGTGG; CCND3 F—CTGACCATCGAAAAACTGTGCAT and R—ACCTCCCAGTCCCGCAA; eIF3a F—TCCAGAGAGCCAGTCCATGC and R—CCTGCCACAATTCCATGCT; eIF3c F—ACCAAGAGAGTTGTCCGCAGTG and R—TCATGGCATTACGGATGGTCC.

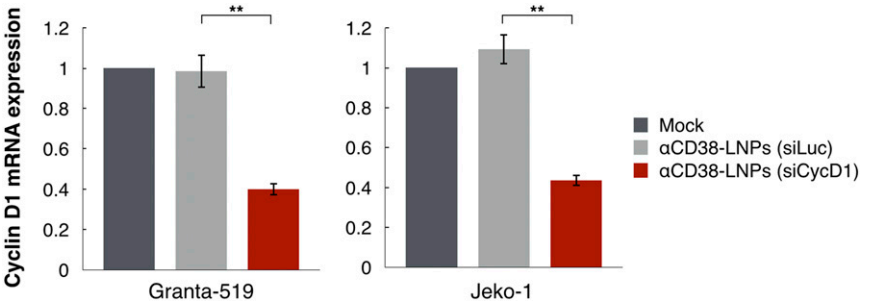

Fig. S1. αCD38-LNPs-siCycD1 mediate cycD1 mRNA knockdown in MCL cell lines. See also Fig. 3 *F* and *G*. qRT-PCR quantification of cyclin D1 transcripts in MCL cell lines. RNA was extracted from cells 48 h following treatment with mock (black), αCD38-LNPs-siLuc (gray), or αCD38-LNPs-siCycD1 (red). Bar plots represent mean ± SEM of cycD1 expression relative to mock ($n = 3$ independent experiments per cell line; $^{**}P < 0.01$; one-way ANOVA test with Bonferroni correction).

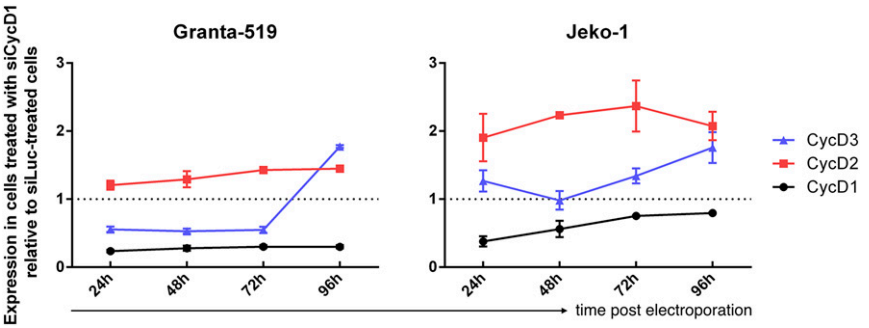

Fig. S2. D-cyclin expression after electroporation with siCycD1. qRT-PCR analysis of CCND1, CCND2, and CCND3 mRNA levels at 24, 48, 72, and 96 h post electroporation in Granta-519 (*Left*) and Jeko-1 (*Right*) cells. Cyclin D2 was consistently overexpressed following treatment with siCycD1. Cyclin D3 exhibited lower or stable expression following treatment before a pronounced increase at day 4 post electroporation. Expression was normalized to both *eIF3a* and *eIF3c* genes and depicted as mRNA concentration relative to cells electroporated with siLuc. Data are mean ± SEM of three independent experiments.

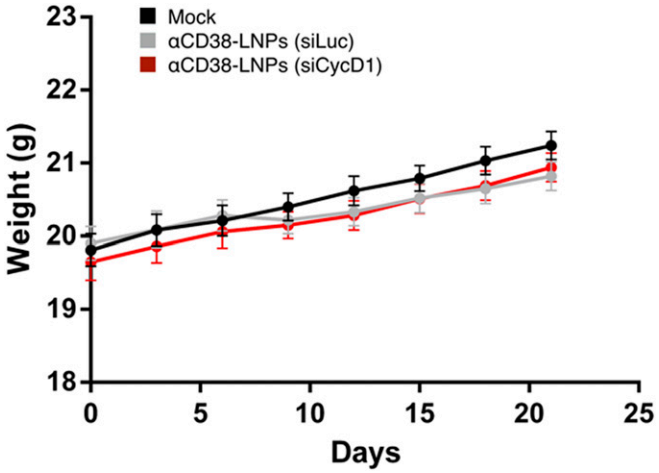

Fig. S3. Repeated i.v. administration of αCD38–LNPs–siRNA did not affect mice body weight. Animals were inoculated and treated as in Fig. 4*C*. Shown are mean weight ± SEM of mice (n = 10 per group).